

Production of Carbon Nanotubes over Fe-FSM-16 Catalytic Material: Effect of Acetylene Flow Rate and CVD Temperature

Journal:	<i>Fullerenes, Nanotubes and Carbon Nanostructures</i>
Manuscript ID:	FNCN1148.R1
Manuscript Type:	Original Article
Date Submitted by the Author:	n/a
Complete List of Authors:	Taş, Sinem; Sabanci University, Faculty of Engineering and Natural Sciences Okyay, Firuze; Sabanci University, Faculty of Engineering and Natural Sciences Sezen, Meltem; Sabanci University, Nanotechnology Research and Application Center Plank, Harald; Graz University of Technology, Institute for Electron Microscopy and Fine Structure Research Yürüm, Yuda; Sabanci University
Keywords:	Carbon Nanotubes, Chemical Vapor Deposition, FSM-16, Fe Catalyst, Acetylene

SCHOLARONE™
Manuscripts

1
2
3
4
5
6
7
8
9
10
11
12
13
14
15
16
17
18
19
20
21
22
23
24
25
26
27
28
29
30
31
32
33
34
35
36
37
38
39
40
41
42
43
44
45
46
47
48
49
50
51
52
53
54
55
56
57
58
59
60

Production of Carbon Nanotubes over Fe-FSM-16 Catalytic Material: Effect of Acetylene Flow Rate and CVD Temperature

Sinem Taş¹, Firuze Okyay¹, Meltem Sezen², Harald Plank³ and Yuda Yürüm^{1*}

¹Faculty of Engineering and Natural Sciences
Sabanci University, Orhanli, Tuzla, Istanbul 34956, Turkey

²Nanotechnology Research and Application Center, Sabanci University, Orhanli, Tuzla
Istanbul 34965, Turkey

³ Institute for Electron Microscopy and Fine Structure Research, Graz University of Technology,
Steyrergasse 17, A-8010 Graz, Austria

*Corresponding Author:

Yuda Yürüm

Faculty of Engineering and Natural Sciences
Sabanci University, Orhanli, Tuzla, Istanbul 34956, Turkey

yyurum@sabanciuniv.edu

Production of Carbon Nanotubes over Fe-FSM-16 Catalytic Material: Effect of Acetylene Flow Rate and CVD Temperature

Sinem Taş¹, Firuze Okyay¹, Meltem Sezen², Harald Plank³ and Yuda Yürüm^{1*}

¹Faculty of Engineering and Natural Sciences
Sabanci University, Orhanli, Tuzla, Istanbul 34956, Turkey

²Nanotechnology Research and Application Center, Sabanci University, Orhanli, Tuzla
Istanbul 34965, Turkey

³ Institute for Electron Microscopy and Fine Structure Research, Graz University of Technology,
Steyrergasse 17, A-8010 Graz, Austria

In this article, a high-yield synthesis of high-quality CNTs using Fe catalysts trapped within channels of Folded Sheet Mesoporous Materials, FSM-16 by Chemical Vapor Deposition CVD using acetylene as a hydrocarbon source is reported. The effect of reaction temperature and acetylene flow rate on the formation of CNTs was investigated. It was found that the yield, diameter and quality of CNTs synthesized strongly depend on reaction temperature during CVD. The resulting materials were characterized by scanning electron microscopy (SEM), Raman spectroscopy, and thermogravimetric analysis (TGA). Our research found that carbon deposition, diameter and quality of the CNTs strongly depend on CVD temperature. However acetylene flow rate did not have any significant effect on diameter distribution. Raman measurement indicated that the synthesized products were MWCNTs. High-resolution transmission electron micrographs of samples reveal the multilayer sidewalls of individual MWCNTs with a diameter of 40 nm, in which hollow and tubal structures were observed.

Keywords Carbon Nanotubes, Chemical Vapor Deposition, FSM-16, Fe Catalyst, Acetylene

Introduction

Discovery of carbon nanotubes (CNT) is an important stepping stone for the nanotechnological progress. Due to the strong knowledge on electrical and mechanical properties of CNTs, they propose many application fields; polymer reinforcements for composites; energy storage; and electronics (1). ~~Because of a strong knowledge on electrical and mechanical properties of CNTs, they find many application fields including polymer reinforcements for~~

1
2
3 ~~composites, energy storage, and electronics~~ (1). However Unfortunately, cost effective
4 production of CNTs is an important issue. Generally, CNTs are synthesized by three different
5 production methods; ~~These are are~~ discharge; laser ablation; and chemical vapor deposition
6 (CVD) ~~methods~~. Both arc discharge and laser ablation methods are very difficult to scale up. On
7 the other hand, due to its simplicity, low cost, ~~product purity~~ and easily controlled growth
8 factors, CVD is the most promising method for industrial scale production of CNTs (2).
9

10
11
12
13
14 Basically, CVD process is dissociation of hydrocarbon molecules on the metal catalyst at
15 high temperatures (500°C-1000°C) for a certain period of time. Precipitation of ~~the~~ carbon on ~~the~~
16 metal particles leads to formation of CNTs. ~~Working conditions of CVD such as~~ Temperature,
17 hydrocarbon concentration, metal particle size, ~~and~~ pretreatment of metallic catalyst, and ~~time of~~
18 ~~the reaction~~ synthesis time are the crucial parameters that affect the quality of final product.
19 Depending on these parameters, single-wall carbon nanotubes (SWCNTs) and multi-wall carbon
20 nanotubes (MWCNTs) can be produced (3). ~~depending on reaction conditions~~ (3).
21

22
23
24
25
26 ~~Because of~~ Since CVD process depends on catalytic decomposition of hydrocarbon
27 molecules, the role of catalyst is important for ability of CNT formation. Metal particle size is
28 crucial for control of CNT diameter. Supported catalysts ensure the control of particle size for
29 the growth process. Ordered mesoporous molecular sieves are preferred as a support material
30 because of high specific surface area, large pore volume, uniform pore structure, and tunable
31 pore size varying from 2 to 10 nm (4). Among the mesoporous materials, FSM-16 is a good
32 candidate because of its large and hexagonal pore structure with high specific surface area.
33 Indeed, ordered structure of FSM-16 ensures the good dispersion of metal particles. When FSM-
34 16 is loaded with metal particles, it can be used as a catalyst for various ~~reactions~~ applications
35 such as, CNT production, hydrogen storage, and adsorption.
36

37
38
39
40
41
42
43
44 To meet the demand for CVD ~~operation~~ process, type of ~~the~~ metal loaded on the support
45 material is critical. In ~~previous~~ earlier studies, researchers reported, ~~transition metals such as Fe,~~
46 ~~Ni, and Co are commonly used~~ that Fe, Ni, and Co are the frequently used transition metals as
47 catalysts for the CNTs production (5). In addition to these, Sc, Ti, V, Cr, Mn, Zn and
48 combination of them are also used as a catalysts (6,7). ~~The performance of catalysis depends~~
49 ~~strongly on the ability of catalytic dissociation of a hydrocarbon molecule~~. 3d metals have also
50 been attractive ~~by~~ means of obtaining nanotubes with better performance. Fe, Ni and Co and
51 their combinations as catalysts offer attractive routes for the synthesis of nanotubes due to the
52
53
54
55
56
57
58
59
60

1
2
3 interactions of their partially filled 3d orbitals with the valence orbitals of the carbon precursors
4
5 (5).

6
7 There are many studies focused on Fe loaded catalysts. Various researchers applied
8 different templates for Fe based catalysis. It is reported that interaction between metal particles
9 and template affects the catalytic activity. Kukovecz et al. (8) obtained MWCNTs with Fe
10 supported on mixtures of Al₂O₃-SiO₂. Many researchers found that Fe loaded SiO₂ is a
11 promising catalyst for MWCNTs synthesis (9-13). Much previous work was oriented towards
12 synthesis of MWCNTs on Fe supported silicon substrate (11-14). Zhao et al. (4) and Atchudan et
13 al. (15) studied MWCNTs synthesis on Fe-MCM-41. However, so far, only Kobayashi et al.
14 reported SWCNTs production over Fe(CH₃COO)₂/Co(CH₃COO)₂ · 4H₂O and Co(NO₃)₂ · 6H₂O
15 impregnated FSM-16 (16). Although the uniformed mesopores could make the catalysts well
16 dispersed in the Fe-FSM-16 molecular sieve, the Fe-FSM-16 catalysts had not been used
17 efficiently to prepare carbon nanotubes with CVD method.
18
19

20
21 In the present study, we report the catalytic activity of Fe impregnated FSM-16 in the
22 production of carbon nanotubes by the CVD method using acetylene as hydrocarbon source. The
23 effect of different reaction temperatures and acetylene flow rate on the formation of CNTs was
24 investigated. The morphology and crystallinity of CNTs grown on Fe-FSM-16 catalyst
25 were investigated using Scanning Electron Microscopy, Raman spectroscopy, and
26 thermogravimetric analysis.
27
28

29 30 31 32 33 34 35 36 37 38 **Experimental**

39 *Synthesis of Fe-FSM-16*

40 According to previously published procedure (17), synthesis of FSM-16 were carried out
41 by using kanemite NaHSi₂O₅·3H₂O and hexadecyltrimethylammonium bromide as a template??.

42
43 ~~A#~~ The impregnation method was described as follows: first the dried powder of as
44 synthesized FSM-16 mixed with iron (III) nitrate nonahydrate (Fe(NO₃)₃·9H₂O), solutions with
45 4 wt % metal loadings. The resultant mixture was stirred at room temperature for 1 hour and then
46 the excess water was removed by stirring at 70°C. The sample was filtered, washed and dried at
47 80°C. Finally, the Fe impregnated sample was calcinated at 550°C for 4 hours in order to remove
48 surfactant.
49
50

51 52 53 54 55 56 *Synthesis of Carbon Nanotubes*

Carbon nanotube production was performed by using a CVD system. 100 mg of the synthesized catalyst was placed into a boat crucible and then put in the middle of the quartz tube (~900 mm in length, 30 mm diameter) of the CVD system to ensure the isothermal conditions. The furnace was heated up to 300°C under 1000 mL/min Ar flow for 30 min to stabilize the catalyst and to purge oxygen present in the furnace prior to the start of the flow of acetylene. Afterwards, the system was set to a temperature between 500°C and 800°C for the CNTs growth. When the temperature set for the experiment was attained, acetylene (40 mL/min) diluted in Ar (1200 mL/min) were introduced into the system. The flow of the acetylene was continued for 30 min in all experiments. The samples were cooled down to room temperature under an Ar atmosphere (1000 mL/min).

To investigate the effect of the flow rate of acetylene the reaction temperature was set to 700°C (as described below the optimum temperature for CNT production) and the acetylene flow rate was changed in the range of 40-120 mL/min.

Carbon nanotube yield was calculated as,

$$\text{Carbon Yield} = \frac{m_{\text{Total C+Catalyst}} - m_{\text{Catalyst}}}{\frac{\text{Flow rate of } C_2H_2 \text{ (l/min)} \times \text{Time (min)}}{22.4 \text{ l/mol of } C_2H_2}} \times 26 \text{ g/mol of } C_2H_2 \times \frac{24 \text{ g of C}}{26 \text{ g of } C_2H_2}$$

where $m_{\text{Total C+Catalyst}}$ is the weight of carbon product and catalyst; m_{Catalyst} is the weight of catalyst used for CNTs growth.

Carbon deposition in an experiment = $m_{\text{Total C+Catalyst}} - m_{\text{Catalyst}}$

Characterization Methods

The synthesized metal-impregnated FSM-16 was characterized by XRD, surface analysis techniques using N₂ adsorption–desorption isotherms. X-ray diffraction pattern were recorded with a Bruker AXS advance powder diffractometer equipped with a Siemens X-ray gun and Bruker AXS Diffrac PLUS software, using Cu Ka radiation ($k = 1.5418$ Angstrom). The samples were scanned in the 2θ range of 2-10°, with step size of 0.01°. Specific surface areas, pore diameters and pore volumes were determined by Quantachrome NOVA 2200 series Surface Analyzer. The nitrogen adsorption/desorption isotherms were recorded at 77 K. Prior to physisorption measurements, the samples were outgassed at 423K for 4h. The specific surface

1
2
3 area and pore volume of the pure and Fe loaded FSM-16 materials were calculated by using the
4 BET and BJH methods.
5
6

7 Different characterization techniques were carried out to examine the CNTs growth on
8 the catalyst particles. The diameter and uniformity of carbon nanotubes were examined with Leo
9 G34-Supra 35VP scanning electron microscope (SEM). The TEM micrographs were acquired by
10 an FEI Tecnai F20 instrument at 200 keV. Thermogravimetric Analysis (TGA) and Raman
11 Spectroscopy were also used to recognize the quality of CNTs as well as amount of defects.
12 Raman spectra of CNT samples were recorded on a Renishaw InVia Reflex Raman Microscopy
13 System (Renishaw Plc.; New Mills, Wotton-under-Edge Gloucestershire, UK) with a 514 nm
14 argon ion laser in the range of 100 to 3200 cm^{-1} . TGA measurements were performed on a
15 Netzsch STA 449 C Jupiter differential thermogravimetric analyzer (precision of temperature
16 measurement $\pm 2^\circ\text{C}$, microbalance sensitivity $\leq 5 \mu\text{g}$) under air atmosphere with a flow rate 50
17 ml/min, at a linear heating rate of $5^\circ\text{C}/\text{min}$.
18
19
20
21
22
23
24
25
26
27

28 **Results and Discussion**

29 *X-ray diffraction pattern of Fe-FSM-16*

30 Figure 1 shows the XRD patterns of FSM-16 and Fe-FSM-16. The peaks were observed
31 in the lower angle region ($2\theta < 10^\circ$), indicated the hexagonal arrays of planes (18). Although
32 both FSM-16 and Fe-FSM-16 have almost the same XRD pattern, the intensity of the observed
33 peaks decreased in the case of Fe-FSM-16. This showed that the ordered structure was partially
34 lost after metal impregnation.
35
36
37
38
39

40 *Nitrogen adsorption–desorption isotherms*

41 Physical adsorption is one of the methods for the porous materials characterization and
42 provides information about surface area, pore size, and pore size distribution. Specific surface
43 area, pore diameter and pore volume data of the FSM-16 and Fe-FSM-16 are presented in Table
44 1. Specific surface area of the FSM-16 and Fe-FSM-16 were $755.1 \text{ m}^2/\text{g}$ and $581.5 \text{ m}^2/\text{g}$,
45 respectively. It seemed that the impregnation of $\text{Fe}(\text{NO}_3)_3 \cdot 9\text{H}_2\text{O}$ on the FSM-16 decreased the
46 surface area due to intrapore formation of ferric oxide. This reduction in the surface area in the
47 case of Fe-FSM-16, were also supported by the lower values of pore diameters (from 3.6 nm to
48 2.5 nm) and pore volumes (from 1.43 cc/g to 0.55 cc/g). In combination with the XRD data,
49 surface area measurements offered detailed information about pore architecture of the catalytic
50
51
52
53
54
55
56
57
58
59
60

1
2
3 material. This is important for the accessibility of active sites and thus is related to the catalytic
4 activity of the Fe-FSM-16.
5

6
7 The N₂ adsorption–desorption isotherms of **FSM-16** and Fe-FSM-16 samples are shown
8 in Figure 2. Samples showed a well defined step at $P/P_0 \approx 0.3\text{--}0.5$, which represented capillary
9 condensation of N₂ gas and uniformity of the pores (19).
10

11 **Effect of temperature on CNTs growth**

12
13
14 Temperature is an important parameter for the growth process, since the ability of a
15 catalyst to dissociate hydrocarbon depends on the reaction temperature. Indeed, raising the
16 reaction temperature increased the carbon formation over the catalysts (12). In order to
17 investigate the temperature effect, experiments were performed between 500°C and 800°C.
18 Figure 3 represents the carbon deposition and the carbon yield with respect to the reaction
19 temperature for all type of catalyst. While carbon yield was 2.88 % at 600°C, it increased to 8 %
20 at 800°C. It was clear that, carbon yield increased with increasing temperature.
21

22
23 Under pyrolytic thermal conditions hydrocarbon molecules broke forming radicallic
24 fragments; these attach to the catalyst particles and diffuse through the catalyst particles, and
25 then led saturation level. During this process, rate determining step is diffusion of carbon from
26 gas/metal interface to metal/carbon interface. As a result, mass flux originated from the solubility
27 difference of carbon at gas/metal interface and metal/carbon interface. At low temperatures
28 carbon solubility in solid solutions was very low (20). Therefore, CNTs structure was not
29 observed at 500°C. Beyond this temperature it seemed that higher amounts of carbon material
30 started to deposit on the catalyst.
31

32
33 Figure 4 illustrates the SEM micrographs of CNTs growth over Fe- FSM-16 at 600°C,
34 700°C and 800°C. From SEM images, it was clear that the growth mechanism of the carbon
35 nanotubes was tip growth. It was obviously observed from the results, that the metal particles
36 were present at the top of the nanotube. Due to weak interaction between the metal particles and
37 the support material, diffused carbon lifted metal particles to top of the nanotube.
38

39
40 Temperature had predominant effect on CNTs growth. Raising the temperature in
41 addition to the increase of the deposited amount of CNTs also affected the morphology of the
42 carbon nanotubes. The effect of increasing the temperature of CVD was observed as an ~~to~~
43 increase in the diameter of CNTs. Diameters of the CNTs produced at 800°C was ~~bigger~~ larger
44 relative to those produced at lower temperatures. Probably, at higher temperatures, catalytic iron
45
46
47
48
49
50
51
52
53
54
55
56
57
58
59
60

1
2
3 species merged on the FSM-16 surface, forming larger catalyst particles that caused to form
4 wider diameter CNTs formation by tip growth (21). Moreover, Zhao et al (4) suggested
5 possibility of acetylene pyrolysis on CNTs sidewalls, leading to tube diameter thickening.
6
7

8
9 Raising the temperature increased the carbon solubility due to enhanced diffusion and
10 this caused the formation of iron carbide at temperatures around 500°C. For the CNTs growth it
11 is essential that iron carbide should decompose and form α -Fe phase. This phase starts to form
12 between 500°C and 725°C and stabilizes at temperatures above 725°C (12). After the formation
13 of α -Fe phase which is the active form for graphite precipitation, the rate of CNTs production
14 increases rapidly. This explained why CNTs did not form at temperatures around 500°C.
15
16

17
18 Although temperature increment led to high CNTs yield, enhanced diffusion of carbon
19 and carbon solubility contributed to increase of average diameter of CNTs. For appropriate yield,
20 the reaction temperature was chosen to be 700 °C.
21
22

23
24 The sample in powder form was investigated at high magnifications using Transmission
25 Electron Microscopy (TEM) in order to analyze the microstructure of CNTs in detail. Bright-
26 field (BF) TEM image in Figure 5 shows the general geometry of nanotubes grown over 4 wt %
27 Fe-FSM-16 particles. High-resolution transmission electron (HRTEM) micrograph in Figure 6
28 reveals the multilayer sidewalls of an individual MWCNT with a diameter of 40 nm, in which
29 hollow and tubal structures were observed.
30
31
32
33
34

35 Effect of Acetylene Flow Rate

36
37 In order to investigate effect of the flow rate of acetylene on the amount of carbon
38 nanotube formed, the experiments were carried out at flow rates of acetylene in the range of 40 -
39 120 mL/min at 700°C with for 30 min reaction time.
40
41

42
43 The carbon deposition and the carbon conversion percentages as a function of acetylene
44 flow rate are given in Figure 7. According to above this analysis (Figure-5), carbon amount
45 deposited on the catalyst increased with increasing flow rate of acetylene up to 80 mL/min.
46 Beyond the flow rate of 80 mL/min the amount of carbon deposition reached to constant values.
47 It seemed that the acetylene flow rate of 80 mL/min was a limiting value for the formation of
48 carbon nanotubes, higher values of acetylene flow did not increase the amount of carbon
49 nanotubes formed. Probably for flow rates greater than 80 mL/min there was no mass flux
50 between acetylene/metal interface since they reached equilibrium. Due to carbon transfer
51
52
53
54
55
56
57
58
59
60

1
2
3 limitations between the hydrocarbon source and the metal interface, carbon conversion might
4 have decreased with increased flow rate of acetylene.
5

6
7 Acetylene flow rate did not have any significant effect on the morphology of the resulting
8 CNTs. The resulting CNTs are shown in Figure 8. It was observed that the diameters of the
9 CNTs ~~diameter was were~~ almost same ~~and it changed~~ in the range of 20-35 nm.
10
11

12 Raman Spectroscopy

13
14 Raman spectroscopy is a powerful tool for the characterization of the synthesized CNTs
15 with respect to their diameter and quality of nanotubes (22). It is possible to distinguish
16 SWCNTs and MWCNTs from each other with the aid of the Raman spectroscopical data. Radial
17 breathing mode (RBM) features appear over lower wavenumber region. RBM modes
18 corresponds coherent vibration of C atoms in radial direction. Raman bands appearing between
19 120-350 cm^{-1} are related to the SWCNTs for diameters in the range of 0.7-2 nm (22,23). The
20 Raman bands at higher wavenumber region are both characteristic for SWCNTs and MWCNTs.
21 The band in the range of 1500-1605 cm^{-1} is referred G band (Graphite Band). G band correspond
22 to vibration of C-C bond of graphene sheet. D band (Disorder Band) is usually observed at in the
23 range 1250-1450 cm^{-1} . D band is the result of disordered-induced vibration of C-C bond. *D/G*
24 peak intensity ratio is an index for determining the CNTs structure (22).
25
26
27
28
29
30
31
32

33 The effect of CVD temperature on the structure of CNTs over 4 wt % Fe-FSM-16 were
34 demonstrated in the Raman spectrum demonstrated in Figure 9. Presence of D and G bands
35 indicated the formation of the ~~that~~ graphitic carbon ~~was formed~~. Since there was not any peak
36 observed in the RBM region, probably the CNTs produced were MWCNTs. While the G band
37 was seen at 1589 cm^{-1} of the carbon nanotubes produced at 600°C, this band appeared at 1592
38 cm^{-1} in the spectra of the products obtained at 700°C and 800°C. The D band position changed
39 from 1341 cm^{-1} (600°C and 700°C) to 1350 cm^{-1} (800°C). Moreover, as the CVD temperature
40 increased, intensities of both D and G band decreased.
41
42
43
44
45
46
47

48 The comparison of the intensity ratios of these two peaks were given in Table 2. It was
49 observed that increasing temperature resulted decrease in the intensity of D and G bands. In the
50 temperature range of 600-800°C, *D/G* peak intensity ratios were 0.81, 0.84, and 0.87. These
51 indicated that the structure of the MWNTs changed with CVD temperature. At higher growth
52 temperatures (700°C and 800°C), D band became stronger and the degree of crystalline
53 perfection of the CNTs decreased. Decomposition of acetylene was very rapid at higher
54
55
56
57
58
59
60

1
2
3 temperatures and this rapid decomposition resulted in excess amorphous carbon formation on the
4 catalyst surface. As a result, excess carbon deactivated the Fe particles and this prevented the
5 growth of perfect CNTs on the catalyst particles.
6
7

8
9 Effect of the acetylene flow rate on the structure of CNTs was also investigated by
10 Raman spectroscopy. Raman spectra of the CNTs formed over 4 wt % Fe-FSM-16 at 40
11 mL/min, 80 mL/min, 100 mL/min, and 120 mL/min acetylene flow rates were shown in Figure
12 9. There was not any peak in the RBM region in the Raman spectrum, this indicated that
13 SWCNTs were not produced but MWCNTs were formed.
14
15

16
17 The ratio of the intensities of *D/G* ratios were shown in Table 3. Intensities of G and D
18 bands increased with increasing acetylene flow rate, however, the ratio of these two band stayed
19 constant indicating that flow rate of acetylene did not have any significant effect on the quality of
20 CNTs.
21
22

23 24 TGA

25
26 TGA measurements were performed in order to investigate the quality of CNTs.
27 Measurements were performed under an air atmosphere with a flow rate 50 ml/min, at a linear
28 heating rate of 5°C/min. TG and DTA curves of samples are shown in Figure 10. It was noted
29 that increasing temperature resulted in weight loss due to burning out of carbon. TG curve
30 exhibited one sequential zone of 375-817°C. Approximately, 60 wt% of the total mass burned
31 out at temperatures below 817°C. According to literature (24, 25), mass loss over the range of
32 300-400°C corresponds to combustion of amorphous carbon and burning of CNTs takes places at
33 400-650°C. Residual mass after the TG experiments obtained in the present work corresponded
34 to 40 wt% of the total mass of the products and this probably contained oxides of the catalytic
35 iron that was together with the carbonaceous products.
36
37
38
39
40
41
42
43

44 The onset, inflection and end temperatures were listed in Table 4. CNTs grown at 600°C,
45 700°C, and 800°C started to burn at 375°C, 436°C, and 518°C, respectively. Weight losses below
46 400°C indicated that burning of amorphous carbon. Graphite particles are more stable compared
47 to amorphous carbon and burned at higher temperatures. With increasing temperature, inflection
48 temperature shifted to higher temperatures. TG-DTA data proved that CNTs grown at higher
49 temperature had better crystalline structure compared to low temperature grown (22).
50
51
52

53 Effect of acetylene flow rate on graphitization of CNTs grown at 700°C was investigated.
54 TG and DTA curves of samples are illustrated in Figure 11. When the flow rate increased from
55
56
57
58
59
60

1
2
3 40 mL/min to 120 mL/min, TG curves exhibited one sequential zone. Furthermore, residual mass
4 was 50 wt% of the total mass. Table 4 revealed the decomposition temperature of formed CNTs.
5
6 It was noted that, the peak of maximum weight loss and inflection temperature shifted toward to
7 higher temperatures with increasing acetylene flow rate. With increasing the flow rate of
8 acetylene above 60 mL/min, inflection temperature did not change. It was found that, for flow
9 rates higher than 60 mL/min, CNTs had better crystalline structure.
10
11
12
13

14 15 16 17 18 **Conclusion**

19 In this study, the effect of CVD temperatures and acetylene flow rates were investigated in the
20 production of CNTs over 4 wt% Fe-FSM-16 catalysts. Catalysts were prepared by wet
21 impregnation method.
22
23

- 24 • Experiments were conducted at 500°C, 600°C, 700°C, and 800°C and the effect of the
25 reaction temperatures was examined for CNT growth. At 500°C, no CNTs grown were
26 observed because of low carbon solubility in metal particles. Higher reaction
27 temperatures contributed to significant amount of carbon deposited on the catalyst and
28 carbon conversion due to enhance diffusion of carbon through the metal particles. It was
29 known that, at higher temperatures, large Fe particles formed and diameter of the CNTs
30 was increase.
31
- 32 • The effect of acetylene flow rate on CNTs production of 4 wt% Fe-FSM-16 at 700°C
33 using 40 mL/min-120 mL/min acetylene flow rate was studied. The carbon amount
34 deposited on the Fe catalyst increased until the acetylene flow rate reached 80 ml/min and
35 it was constant with increasing flow rate. This behavior was the result of equilibrium of
36 carbon concentrations between acetylene/metal interfaces. Moreover, SEM images
37 demonstrated that CNTs diameter was almost same with increasing acetylene flow rate.
38
- 39 • **High-resolution transmission electron micrographs of samples reveal the multilayer
40 sidewalls of individual MWCNTs with diameter of 40 nm, in which hollow and tubal
41 structures were observed.**
42
- 43 • Raman spectroscopical results clearly indicated that the CNTs produced were MWCNTs.
44 Some of the formed CNTs were also examined by TGA for having an idea about quality
45 of CNTs. Thermal decomposition differences were observed during the burning of CNTs.
46
47
48
49
50
51
52
53
54
55
56
57
58
59
60

1
2
3 At low temperatures, CNTs started decomposition below 400°C due to burning of
4 amorphous carbon. As the CVD, temperature increased, samples contained less
5 amorphous carbon and more CNTs thus burning temperatures shifted toward to higher
6 temperatures. On the other hand, TGA results supported the Raman results for CNT
7 production under different acetylene flow rate. It was found that, inflection temperature
8 was almost same.
9
10
11
12
13

14 15 16 **Acknowledgements**

17 This work was supported by the Scientific and Technological Research Council of
18 Turkey (TUBITAK) with the Project No. 109M214.
19

20
21 High-resolution transmission electron micrographs of samples were kindly recorded by
22 Prof. Dr. Christian Gspan of Institute for Electron Microscopy and Fine Structure Research, Graz
23 University of Technology, Steyrergasse, Graz, Austria.
24
25
26
27
28
29

30 31 **References**

- 32 1. Popov V.N. (2004) Carbon nanotubes: properties and application. *Materials Science &*
33 *Engineering R-Reports*, 43: 61.
- 34 2. Somanathan T., Pandurangan, A. and Sathiyamoorthy D. (2006) Catalytic influence of
35 mesoporous Co-MCM-41 molecular sieves for the synthesis of SWNTs via CVD method.
36 *Journal of Molecular Catalysis A-Chemical*, 256: 193.
- 37 3. Paradise M. and Goswami T. (2007) Carbon nanotubes - Production and industrial
38 applications. *Materials & Design*, 28: 1477.
- 39 4. Zhao, Q., LiY.H., Zhou X.P., Jiang T.S., Li C.S., and Yin H.B. (2010) Synthesis of
40 multi-wall carbon nanotubes by the pyrolysis of ethanol on Fe/MCM-41 mesoporous
41 molecular sieves. *Superlattices and Microstructures*, 47: 432.
- 42 5. Oncel Ç. and Yürüm Y. (2006) Carbon nanotube synthesis via the catalytic CVD method:
43 A Review on the Effect of Reaction. *Parameters, Fullerenes, Nanotubes and Carbon*
44 *Nanostructures*, 14: 17-37.
- 45 6. Shanov V., Yun Y., Shulz M.J. (2006) Synthesis and characterization of carbon nanotube
46 materials. *Journal of University of Chemical Technology and Metallurgy*, 41: 377.
47
48
49
50
51
52
53
54
55
56
57
58
59
60

- 1
 - 2
 - 3
 - 4
 - 5
 - 6
 - 7
 - 8
 - 9
 - 10
 - 11
 - 12
 - 13
 - 14
 - 15
 - 16
 - 17
 - 18
 - 19
 - 20
 - 21
 - 22
 - 23
 - 24
 - 25
 - 26
 - 27
 - 28
 - 29
 - 30
 - 31
 - 32
 - 33
 - 34
 - 35
 - 36
 - 37
 - 38
 - 39
 - 40
 - 41
 - 42
 - 43
 - 44
 - 45
 - 46
 - 47
 - 48
 - 49
 - 50
 - 51
 - 52
 - 53
 - 54
 - 55
 - 56
 - 57
 - 58
 - 59
 - 60
7. Dumanli A. and Yürüm Y. (2011) Carbon nanotube and nanofiber growth on Zn-based catalysts. *Fullerenes, Nanotubes, and Carbon Nanostructures*, 19: 155.
8. Kukovecz A., Konya Z., Nagaraju N., Willems I., Tamasi A., Fonseca A., Nagy J. B., Kiricsi I. (2000) Catalytic synthesis of carbon nanotubes over Co, Fe and Ni containing conventional and sol-gel silica-aluminas. *Physical Chemistry Chemical Physics*, 2: 3071.
9. Hernadi K., Fonseca A., Nagy J.B., Siska A., Kiricsi I. (2000) Production of nanotubes by the catalytic decomposition of different carbon-containing compounds. *Applied Catalysis A: General*, 199: 245.
10. Duesberg G.S., Graham A.P., Liebau M., Seidel R., Unger E., Kreupl F., Hoenlein W. (2003) Growth of isolated carbon nanotubes with lithographically defined diameter and location. *Nano Letters*, 3: 257.
11. Klinke C., Bonard J.M., Kern K. (2001) Comparative study of the catalytic growth of patterned carbon nanotube films. *Surface Science*, 492: 195.
12. Ermakova M.A., Ermakov D.Y., Chuvilin A.L., Kuvshinov G. (2001) Decomposition of methane over iron catalysts at the range of moderate temperatures: The influence of structure of the catalytic systems and the reaction conditions on the yield of carbon and morphology of carbon filaments. *Journal of Catalysis*, 201: 183.
13. Venegoni D., Serp P., Feurer R., Kihn Y., Vahlas C., Kalck P. (2002) Parametric study for the growth of carbon nanotubes by catalytic chemical vapor deposition in a fluidized bed reactor. *Carbon*, 40: 1799.
14. Cho Y.S., Choi G.S., S. Hong Y., Kim D. (2002) Carbon nanotube synthesis using a magnetic fluid via thermal chemical vapor deposition. *Journal of Crystal Growth*, 243: 224.
15. Atchudan R., Pandurangan A., Somanathan T. (2009) Bimetallic mesoporous materials for high yield synthesis of carbon nanotubes by chemical vapor deposition techniques. *Journal of Molecular Catalysis A-Chemical*, 309: 146.
16. Kobayashi K., Kitaura R., Kumai Y., Goto Y., Inagaki S., Shinohara H. (2009) Fabrication of single-wall carbon nanotubes within the channels of a mesoporous material by catalyst-supported chemical vapor deposition. *Carbon*, 47: 722.
17. Inagaki S., Sakamoto Y., Fukushima Y., Terasaki O. (1996) Pore wall of a mesoporous molecular sieve derived from kanemite. *Chem. Mater*, 8: 2089.

- 1
2
3
4
5
6
7
8
9
10
11
12
13
14
15
16
17
18
19
20
21
22
23
24
25
26
27
28
29
30
31
32
33
34
35
36
37
38
39
40
41
42
43
44
45
46
47
48
49
50
51
52
53
54
55
56
57
58
59
60
18. Inagaki S., Koiwai A., Suzuki N., Fukushima Y., and Kuroda K. (1996) Syntheses of highly ordered mesoporous materials, FSM-16, derived from kanemite. *Bulletin of the Chemical Society of Japan*, 69: 1449.
 19. Ghattas M. S. (2006) Cobalt modified mesoporous FSM-16 silica: Characterization and catalytic study. *Microporous and Mesoporous Materials*, 97: 107.
 20. Pollack H. W. (1988) *Materials Science and Metallurgy*, Prentice Hall.
 21. Kukovitsky E.F., L'vov S.G., Sainov N.A., Shustov V.A., Chernozatonskii L.A. (2002) Correlation between metal catalyst particle size and carbon nanotube growth. *Chemical Physics Letters*, 355: 497.
 22. Chen C.M., Dai Y.M., Huang J.G., Jehng J.M. (2006) Intermetallic catalyst for carbon nanotubes (CNTs) growth by thermal chemical vapor deposition method. *Carbon*, 44: 1808.
 23. Dresselhaus M.S., Dresselhaus G., Saito R., Jorio A. (2005) Raman spectroscopy of carbon nanotubes. *Physics Reports-Review Section of Physics Letters*, 409: 47.
 24. Scaccia S., Carewska M., Prosini P.P. (2005) Study of purification process of single-walled carbon nanotubes by thermoanalytical techniques. *Thermochimica Acta*, 435: 209.
 25. Lee C.J., Park J., Huh Y., Lee J.Y. (2001) Temperature effect on the growth of carbon nanotubes using thermal chemical vapor deposition. *Chemical Physics Letters*, 343:33.

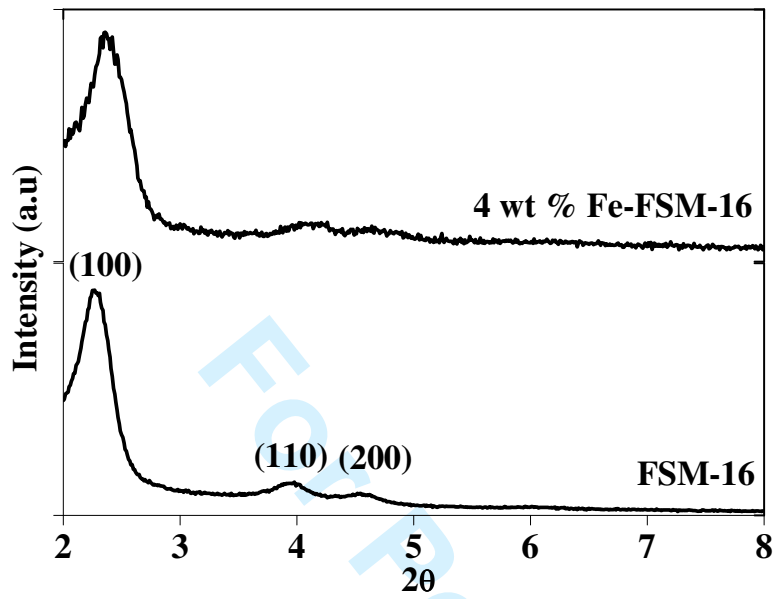


Figure 1. XRD pattern of FSM-16 and Fe impregnated FSM-16.

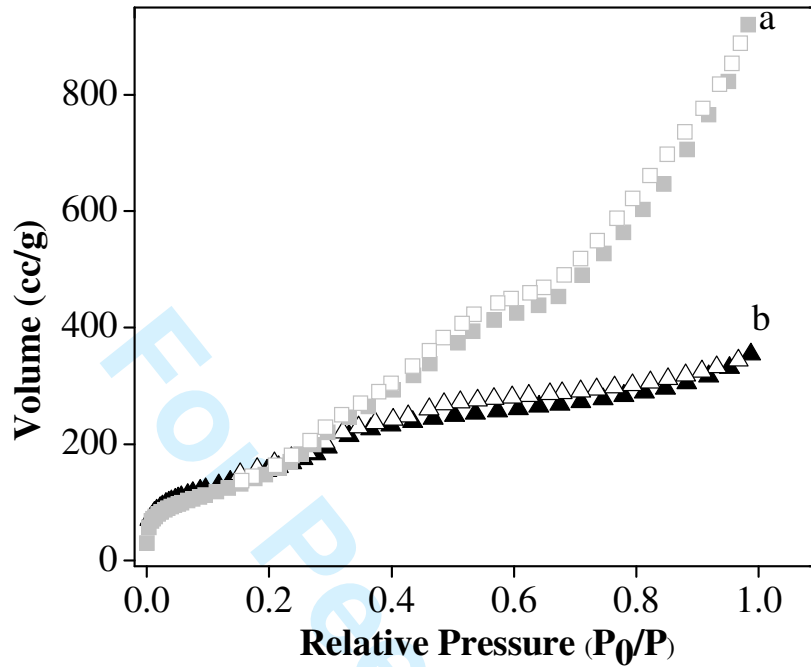


Figure 2. Adsorption-desorption isotherms for (a) FSM-16 and (b) 4 wt % Fe-FSM-16

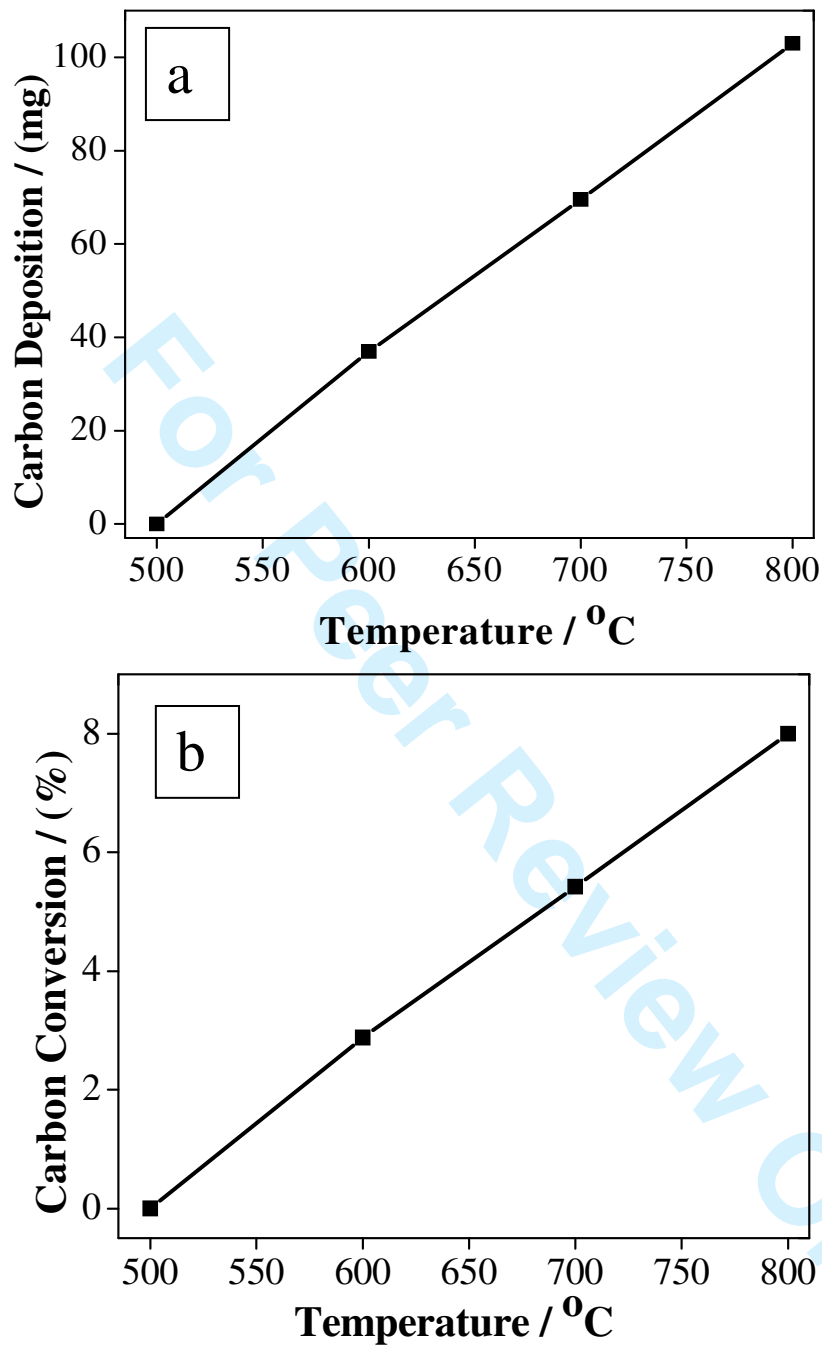


Figure 3. a) Carbon deposition and b) Carbon conversion change as a function of reaction temperature.

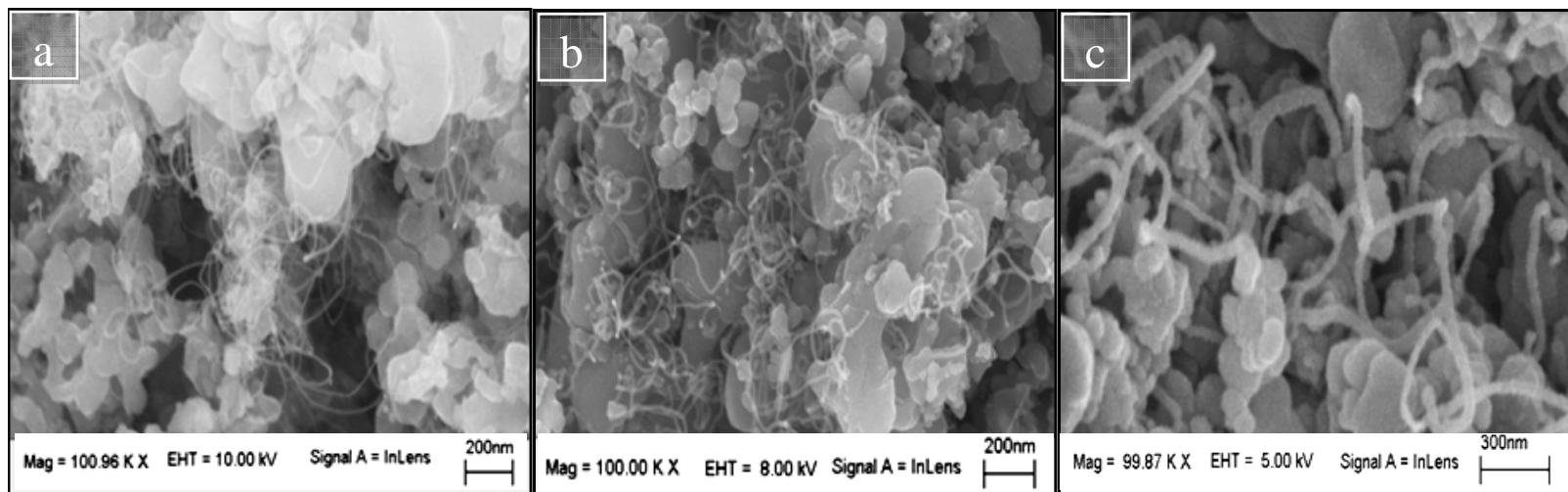


Figure 4. CNTs growth over 4 wt % FSM-16 at (a) 600°C, (b) 700°C, (c) 800°C.

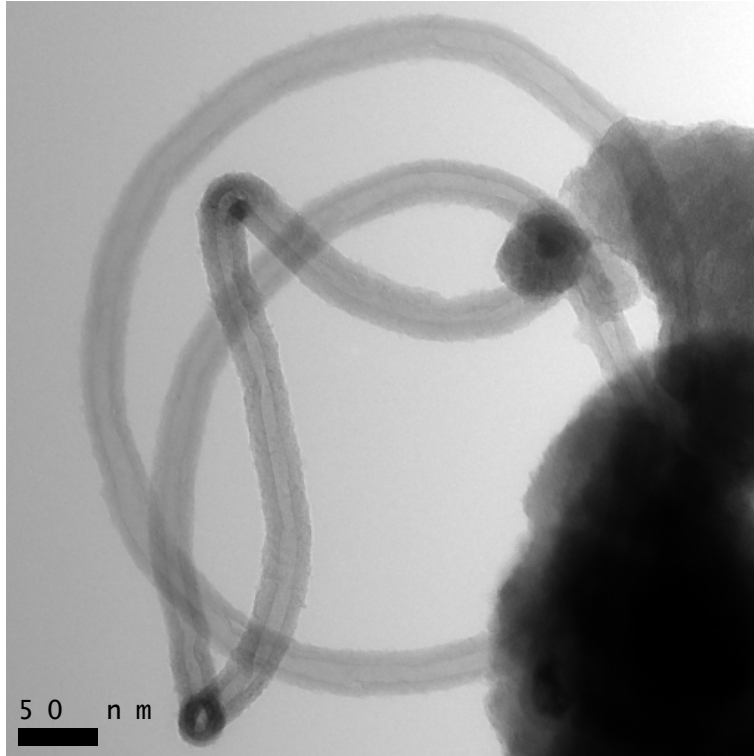


Figure 5. Multi-walled carbon nanotubes grown over 4 wt % Fe-FSM-16 particles.

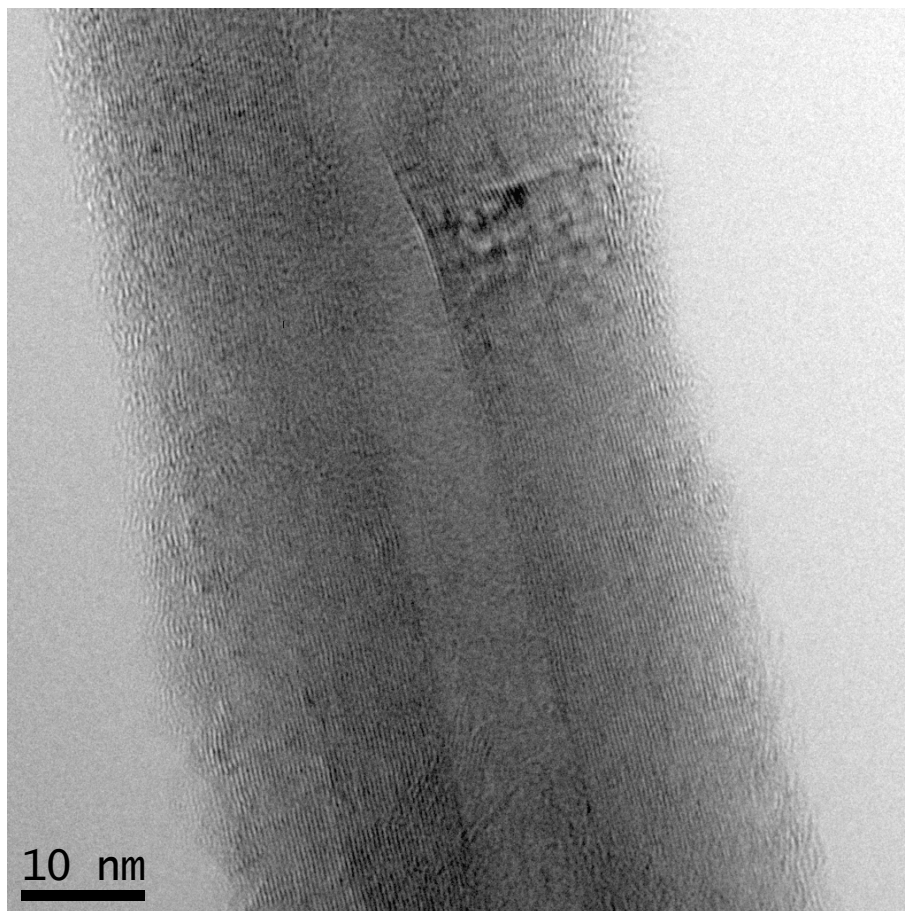


Figure 6. HRTEM micrograph of an individual multi-walled carbon nanotubes.

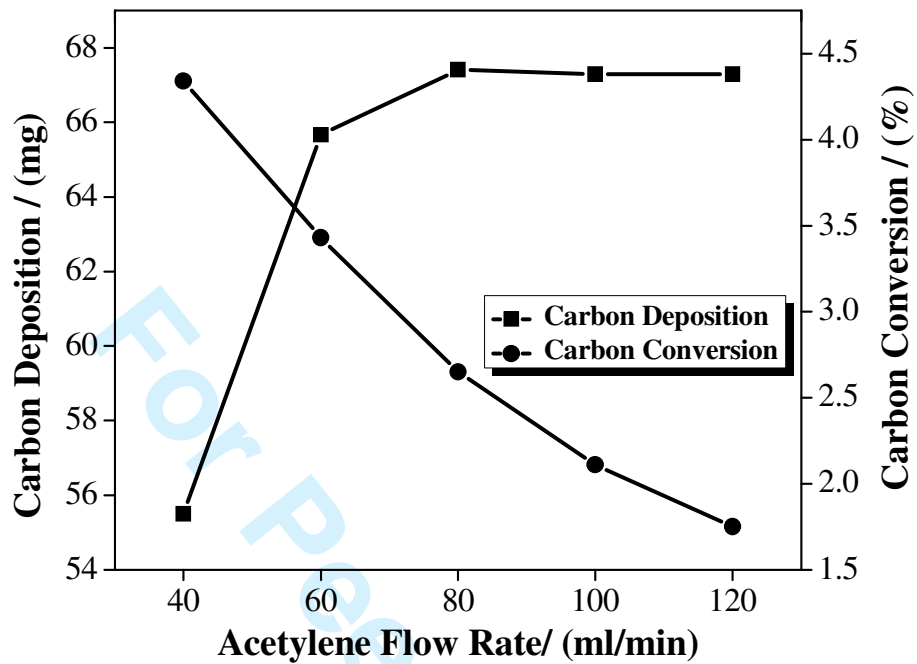


Figure 7. Carbon deposition and conversion change as a function of acetylene flow rate.

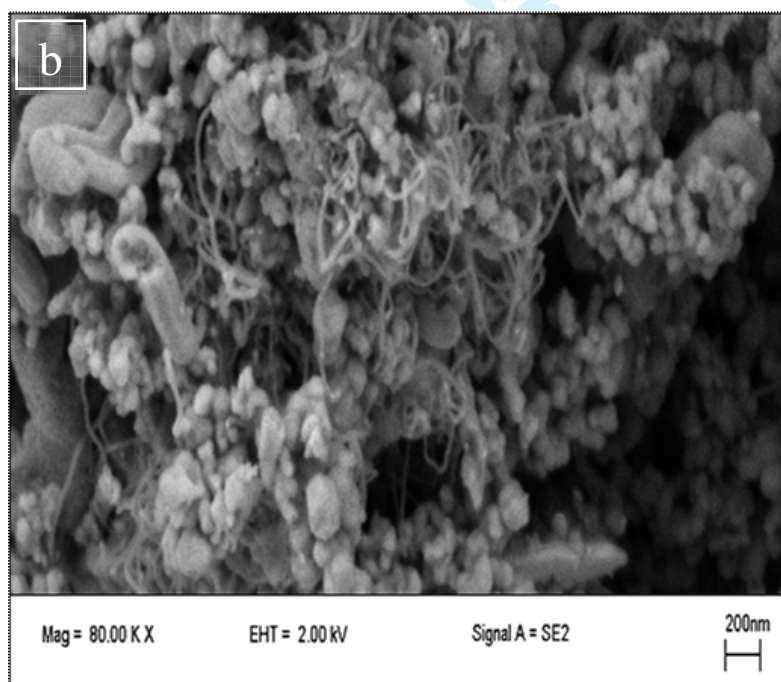
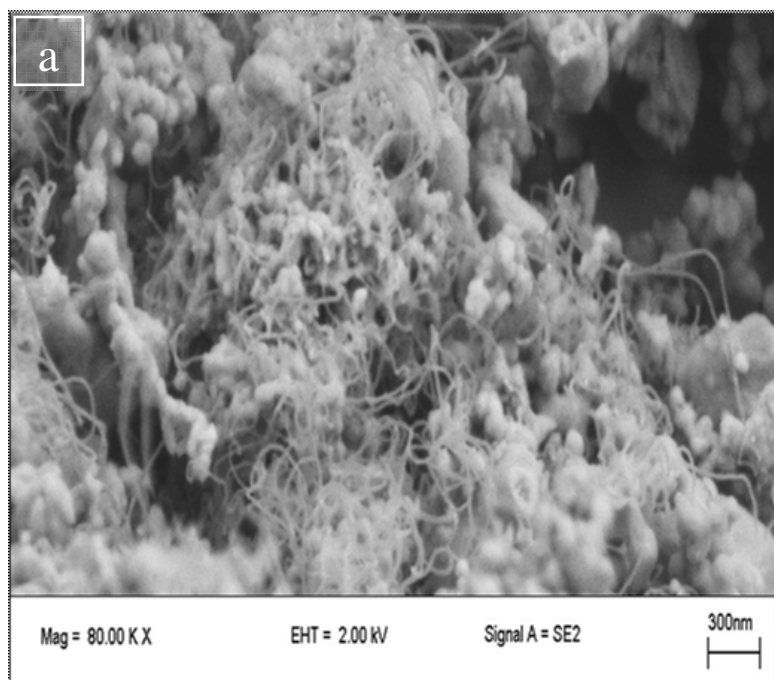


Figure 8. CNTs growth over 4 wt % Fe- FSM-16 with a) 80 ml/min acetylene flow rate, b) 120 ml/min acetylene flow rate.

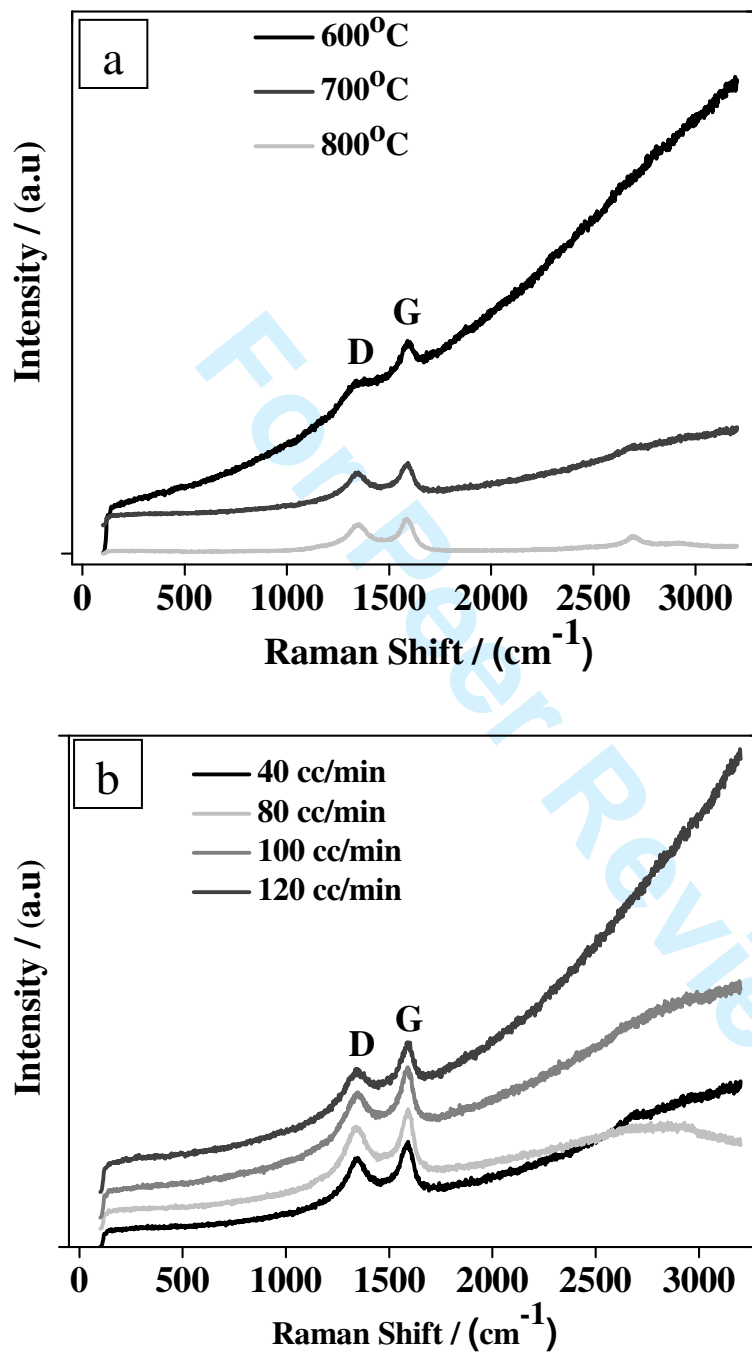


Figure 9. Raman spectra of carbon deposits on 4 wt % Fe-FSM-16, a) Effect of reaction temperature, b) Effect of acetylene flow rate.

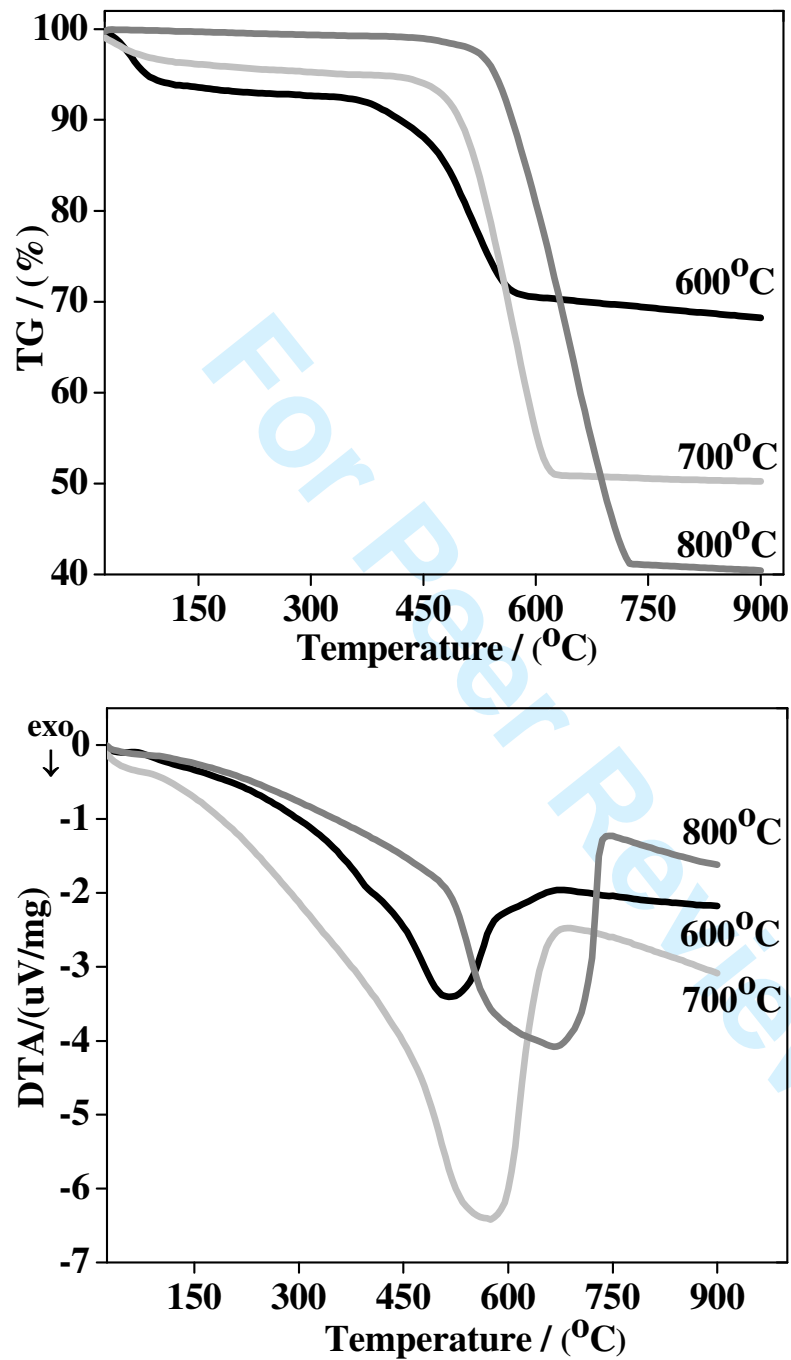


Figure 10. TGA thermograms and DTA curves of CNTs.

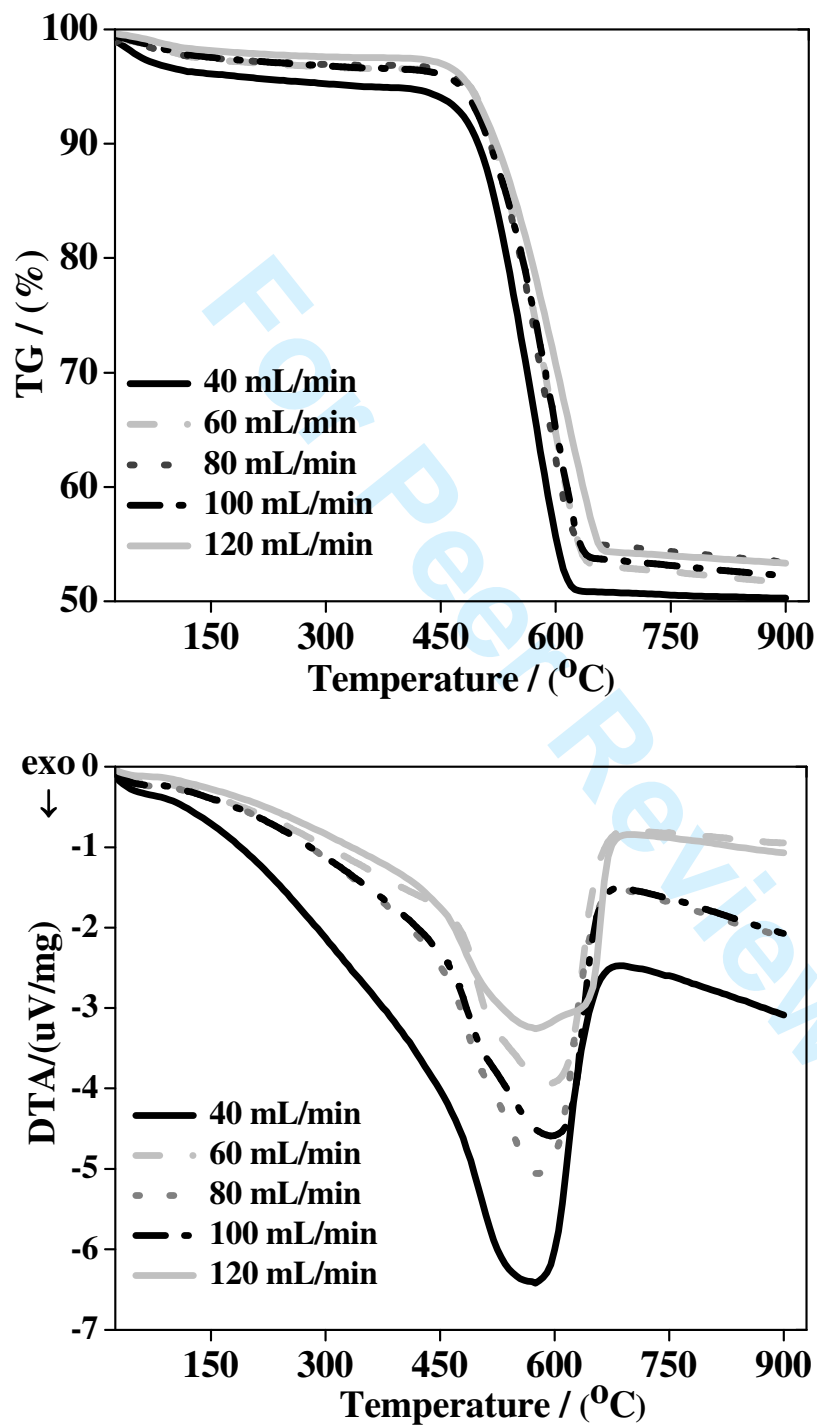


Figure 11. TGA thermograms and DTA curves of growth of CNTs with various acetylene flow rate.

Tables

Table 1. Results of specific surface area, pore size and pore volume of catalysts.

Sample	Specific Surface Area (m ² /g)	Average Pore Diameter (nm)	Total Pore Volume (cc/g)
FSM-16	755.1	3.6	1.43
4 wt % Fe- FSM-16	581.5	2.5	0.55

Table 2. Parameters of D and G band for carbon deposits on 4 wt % Fe -FSM-16 at different temperature

Temperature	Raman Shift (cm ⁻¹) (D-Band)	Raman Shift (cm ⁻¹) (G-Band)	Absolute Intensity (D-Band)	Absolute Intensity (G-Band)	I _D /I _G
600°C	1341	1589	7981	9824	0.81
700°C	1341	1592	2426	2880	0.84
800°C	1350	1592	1378	1589	0.87

Table 3: Parameters of D and G band for carbon deposits on 4 wt % Fe -FSM-16 produced with different acetylene flow rates at 700°C

Flow Rate	Raman Shift (cm ⁻¹) (D-Band)	Raman Shift (cm ⁻¹) (G-Band)	Absolute Intensity (D-Band)	Absolute Intensity (G-Band)	I _D /I _G
40 mL/min	1341	1592	2426	2880	0.84
80 mL/min	1356	1579	2550	3060	0.83
100 mL/min	1358	1585	3380	4093	0.83
120 mL/min	1356	1595	3335	4004	0.83

Table 4. Onset, inflection and end temperature obtained from DTG curve

Sample	Onset Temperature	Inflection Temperature	End Temperature
CNTs-600°C	375	513	666
CNTs-700°C (40 mL/min)	436	573	686
CNTs-800°C	518	666	817
CNTs-60 mL/min	449	591	700
CNTs-80 mL/min	431	578	726
CNTs--100 mL/min	443	597	724
CNTs-120 mL/min	446	573	713